NJC

PAPER

View Article Online
View Journal | View Issue

Cite this: *New J. Chem.*, 2019, **43**, 3899

Fluorescence sensing and intracellular imaging of Pd^{2+} ions by a novel coumarinyl-rhodamine Schiff base†

Arup Kumar Adak,[ab] Rakesh Purkait,[b] Saikat Kumar Manna,[c] Bankim Chandra Ghosh,[d] Sudipta Pathak[c] and Chittaranjan Sinha *[b]

Received 26th December 2018,
Accepted 26th January 2019

DOI: 10.1039/c8nj06511j

rsc.li/njc

Coumarinyl-rhodamine, **HCR**, served as an extremely selective sensor for Pd^{2+} ions in ethanol/H_2O (8 : 2, v/v, HEPES buffer, pH 7.2) solution and the limit of detection (LOD) was 18.8 nM (3σ method). The free sensor, **HCR**, was weakly emissive and in the presence of Pd^{2+}, the colour changed from straw to pink with very strong emission at 598 nm in the presence of eighteen other cations. A plausible mechanism involved opening of the spirolactam ring of rhodamine on interaction with Pd^{2+}, which was justified by structure optimization and transition energy calculations using the DFT technique. **HCR** underwent 1 : 1 complexation with Pd^{2+}, which was confirmed *via* the Job's plot, mass spectra and Benesi–Hildebrand plot (association constant K_a, 9.1 × 10^4 M^{-1}). A separate *in vitro* experiment showed that **HCR** could specifically sense Pd^{2+} in MCF7 (human breast adenocarcinoma) cell lines.

1. Introduction

In the last few years, the development of methods for the identification and sensing of platinum group metals (PGMs) has received considerable interest because of their enormous biological, environmental, industrial and chemical significance.[1–4] Among these, palladium, a precious metal, has become one of the most attractive sensing targets in recent years because of its wide catalytic use in the synthesis of organic and pharmaceutical molecules, fuel cells, dental appliances, medical devices, electrical equipments, *etc.*[5,6] In the Pd-catalysed reactions, either the Pd(0) may be temporarily oxidized or Pd(IV) may be reduced to Pd(II) during the reactions. The final product is often contaminated with a Pd(II) impurity even after rigorous purification. Such contamination at an ultratrace level in industrial products may cause serious health problems. Due to its thiophilic nature, palladium can bind with DNA, proteins and other macromolecules and disturb a variety of cellular processes.[7,8] Moreover, palladium also hinders the activity of many enzymatic reactions such as those of alkaline phosphatase, creatine kinase and prolyl hydroxylase (hypoxia-inducible factor).[9,10] Therefore, various analytical techniques are used for the quantitative analysis of palladium. Popular techniques include inductively coupled plasma-mass spectrometry (ICP-MS), atomic absorption spectrometry (AAS), solid-phase microextraction high performance liquid chromatography (SPME-HPLC) and X-ray fluorescence spectroscopy.[11–13] However, these methods require sophisticated highly expensive equipments, extensive sample preparation steps, and time-consuming and high salaried experts. Among these different techniques used for the analysis of palladium ions, colorimetric and fluorometric techniques are more convenient and dependable for the rapid and sensitive detection of palladium both qualitatively and quantitatively because of their simplicity, selectivity and sensitivity. Hence, the development of palladium-selective fluorescent probes is extremely essential. Pd^{2+}, being a heavy transition metal ion with open shell electronic configuration, is a typical fluorescence quencher.[14] Based on the ON–OFF[15] or OFF–ON[16,17] mechanism, some fluorescent chemosensors and chemodosimeters are synthesized for identifying palladium species. For the design of a sensor, the important objectives are long-wavelength emission and ecofriendly availability of fluorescent chemosensors. Thus, rhodamine-functionalized chemosensors are receiving considerable interest in current years.[18] For the last couple of years, we have considered a strategy to design rhodamine derivatives for the identification of trace levels of Pd; allyl ether Schiff base of rhodamine[19] was tested for the detection of total Pd at 50 nM, while allyl ether hydrazone rhodamine could detect as low as 95 nM concentration[20] at pH 7.2. The performance of rhodamine derivatives inspired us to synthesize newer

[a] *Department of Chemistry, Bidhannagar College, EB-2, Sector – 1, Salt Lake, Kolkata-700064, West Bengal, India*
[b] *Department of Chemistry, Jadavpur University, Kolkata-700032, West Bengal, India. E-mail: crsjuchem@gmail.com*
[c] *Department of Chemistry, Haldia Govt. College, Debhog, Haldia, Purba Medinipur-721657, West Bengal, India*
[d] *Department of Chemistry, Durgapur Govt. College, J. N. Avenue, Durgapur, Paschim Barddhaman-713214, West Bengal, India*

† Electronic supplementary information (ESI) available. See DOI: 10.1039/c8nj06511j

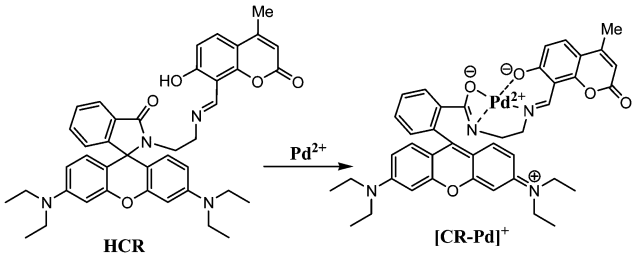

Scheme 1 Proposed sensing mechanism of Pd^{2+}-selective sensor **HCR** (λ_{em} = 598 nm for the complex).

chemosensors, which can detect even lower concentrations of Pd(II). For further accomplishment, we selected two fluorogenic units, coumarin and rhodamine, to combine into a single molecule, (*E*)-3′,6′-bis(diethylamino)-2-(2-(((7-hydroxy-4-methyl-2-oxo-2*H*-chromen-8-yl)methylene)amino)ethyl)spiro[isoindoline-1,9′-xanthen]-3-one (**HCR**) (Scheme 1); it was used for the detection of Pd^{2+}. **HCR** was nearly non-emissive, while its complexation with Pd^{2+} resulted in a powerfully fluorescent motif within the red wavelength region (598 nm), which may be due to opening of the spirolactam ring of rhodamine. The potential application of the ligand (**HCR**) was carried out by intracellular imaging in the MCF7 (human breast adenocarcinoma) cell line in the presence of exogenous palladium ions.

2. Experimental section

2.1 Materials and methods

Rhodamine B (Sigma-Aldrich), resorcinol, ethylene diamine, and ethyl acetoacetate (Spectrochem) were used as received. All other organic chemicals and inorganic salts were acquired from Merck and utilized without further purification. Purified water was collected from Milli-Q water (Millipore). Following instruments were used for different physicochemical measurements: Perkin-Elmer 2400 Series-II CHN analyzer, Perkin Elmer, USA for elemental analyses; Perkin Elmer Lambda 25 spectrophotometer for absorption spectral measurements; Perkin Elmer spectrofluorimeter model LS55 for emission spectral studies; Perkin Elmer LX-1 FTIR spectrophotometer for obtaining IR spectra; Bruker (AC) 300 MHz FT-NMR spectrometer utilizing TMS as an internal standard for NMR spectra; and Water HRMS model XEVO-G2QTOF#YCA351 spectrometer for mass spectra. Data were collected at room temperature.

The test sample and reference were excited at identical wavelength. From the area of the fluorescence spectra (using available software in the instrument), the fluorescence quantum yield of the experimental sample was calculated using the following equation:

$$\frac{\phi_S}{\phi_R} = \left[\frac{F_S}{F_R}\right] \times \left[\frac{A_R}{A_S}\right] \times \left[\frac{\eta_S{}^2}{\eta_R{}^2}\right] \quad (1)$$

Here, ϕ_R and ϕ_S are the fluorescence quantum yields of the reference and samples; F_R and F_S are the areas under emission spectra of the reference and sample, A_R and A_S are absorbances of reference and sample at the excitation wavelength, η_R and η_S are the refractive indices of the solvent used for the reference and the sample, respectively. Fluorescein (reported quantum yield, ϕ_R = 0.79 in 0.1 M NaOH)[21] was used as a reference sample.

2.2 Synthesis of probe HCR

4-Methyl-7-hydroxy-8-formylcoumarin (**A**)[22] and *N*-(rhodamine-B)lactam-1,2-ethylenediamine (**B**)[23] were synthesized using previously reported methods. A suspension of **B** (1.0 equiv.) in dry EtOH (10 mL) was stirred at 80 °C with 4-methyl-7-hydroxy-8-formyl coumarin (**A**) (1.0 equiv.) in the same solvent (10 mL) under an inert (N_2) environment for 2 h; an orange-yellow colored crystalline product was separated. Solvent extraction using ethyl acetate/brine water system was performed followed by chromatographic separation over silica gel using ethyl acetate/petroleum ether (1 : 1 v/v) solvent mixture to elute the desired product **HCR**. Yield: 75%, m.p.: 145–147 °C, ^{1}H NMR (300 MHz, $CDCl_3$) δ 8.62 (s, 1H), 7.91 (d, J = 5 Hz, 1H), 7.44–7.42 (m, 3H), 7.09 (t, J = 3 Hz, 1H), 6.70 (d, J = 9 Hz, 1H), 6.32–6.45 (m, 6H), 5.98 (s, 1H), 3.51 (t, J = 6 Hz, 2H), 3.32–3.34 (m, 10H), 2.42 (s, 3H), 1.16 (t, J = 6.81 Hz, 12H) (ESI,† Fig. S1); ^{13}C NMR (75 MHz, $CDCl_3$) δ 172.4, 168.3, 162.3, 160.6, 160.5, 155.0, 153.6, 153.4, 153.3, 148.9, 132.6, 130.8, 129.5, 128.7, 128.1, 123.8, 123.0, 117.7, 109.2, 108.3, 105.2, 105.0, 97.7, 64.9, 53.5, 44.4, 40.1, 18.9, 12.6. (ESI,† Fig. S2); MS ES$^+$, m/z calculated for $C_{41}H_{42}N_4O_5$: 670.32; found: 671.16 $[M + H]^+$ (ESI,† Fig. S3); IR (KBr pellet, cm^{-1}): 3444, 1614 (ESI,† Fig. S4).

2.3 UV-Vis and fluorescence spectral studies

Ethanol solution (5 mL) of **HCR** (3.35 mg, 0.001 mmol) was used as stock solution; 100 μL of this stock of **HCR** was diluted utilizing 2 mL ethanol/H_2O (8 : 2, v/v) containing HEPES buffer (pH 7.2). Independently, a Pd^{2+} solution was prepared by warming $PdCl_2$ (1.77 mg, 0.001 mmol) in minimum volume of DMSO and diluted to 10 mL by adding water. Microlitre quantities of Pd^{2+} solution were slowly poured into the above-mentioned **HCR** solution for spectral measurement. Excitation wavelength of 545 nm (excitation slit = 5.0 and emission slit = 5.0) was used for fluorescence study.

2.4 Theoretical computation

Optimized molecular geometries of **HCR** and $[\mathbf{CR}^-\text{-}Pd^{2+}]^+$ complex were generated using the DFT/B3LYP technique by exploiting the Gaussian 09 software.[24–27] For C, H, N, and O, basis set of 6-311G was used and for heavy atom Pd, the LanL2DZ basis set was used.[28,29] Vibrational frequency calculations were verified using optimized geometries, which represented the structures of the species closer to the actual structure. TD-DFT technique in MeOH using conductor-like polarizable continuum model (CPCM)[30–32] was employed for theoretical evaluation of UV-Vis spectra. The fractional contributions of various groups to the molecular orbital were checked by the GAUSSSUM program.[33]

2.5 Biological studies

2.5.1 Cell culture. The cells of MCF7, human breast adenocarcinoma cell line (NCCS, Pune, India), were cultured in a

CO_2-incubator (5%) at 37 °C using DMEM containing fetal bovine serum (FBS) (10%), kanamycin sulfate (110 mg L^{-1}), penicillin (50 units per mL) and streptomycin (50 μg mL^{-1}). The cell detachment during cell splitting program was checked by Trypsin-EDTA (1×) solution, which was used for cell detachment during cell splitting.

2.5.2 Cell viability assay of tetramer peptides. Human breast adenocarcinoma cell line, *i.e.*, MCF7 cells were taken in the DMEM culture media using 10% fetal bovine serum. At different concentrations of **HCR** ligand in DMEM medium, cell viability assay was performed within ninety-six-well plates. MTT (3-(4,5-dimethylthiazol-2-yl)-2,5-diphenyltetrazolium bromide) is a colorimetric technique, where a yellow tetrazole compound gets reduced to purple-coloured formazan by reductase enzymes present in living cells, while dead cells cannot interfere. Moreover, formazan was further dissolved in DMSO/MeOH (1 : 1 (v/v)) and absorbance of each well was measured at 550 nm using a micro-plate ELISA reader. The percentage of viability was measured from the absorbance value. Percentage viability was calculated as follows:

$$\frac{\{A_{550}(\text{treated cell}) - A_{550}(\text{background})\}}{\{A_{550}(\text{untreated cell}) - A_{550}(\text{background})\}} \times 100.$$

2.5.3 Cellular uptake study by microscopic imaging. Approximately, 2000 MCF7 cells were seeded in DMEM medium containing 10% fetal bovine serum on a cover glass bottom disc overnight before treatment. Then, the media were removed and 5 μM **HCR** was added in DMEM-containing media and incubated for 3 h (DMSO concentration was maintained at 0.4%). After 3 h of incubation, 5 μM of Pd^{2+} was added and incubated for another 30 min followed by the addition of 4% formaldehyde in PBS buffer for 30 min to fix the cells in each cover glass. Formaldehyde solution was then removed and washed with PBS buffer. Cell imaging was performed by a spinning disc confocal microscope with 40× objective (Olympus) equipped with an AndoriXon 3897 EMCCD camera in 568 nm wavelength light.

3. Results and discussions

3.1 Synthesis and characterization of HCR

The probe (*E*)-3′,6′-bis(diethylamino)-2-(2-(((7-hydroxy-4-methyl-2-oxo-2*H*-chromen-8-yl)methylene)amino)ethyl)spiro[isoindoline-1,9′-xanthen]-3-one (**HCR**) was synthesized using the reaction of 4-methyl-7-hydroxy-8-formyl-coumarin (**A**) and *N*-(rhodamine-B)lactam-1,2-ethylenediamine (**B**) (ESI,† Scheme S1). In the FTIR spectrum of **HCR**, ν(CHO) [at 1651 cm^{-1}] of **A** and $\nu(NH_2)$ [at 3225 cm^{-1}] of **B** remain absent and new peak appears at 1614 cm^{-1} which is due to ν(C═N). This observation substantiates that condensation of **A** and **B** has occurred to give the product **HCR**. A mass spectral peak at 671.16 matched $[M + H]^+$ (calculated *m*/*z* for $C_{41}H_{42}N_4O_5$ is 670.32) and supported the elemental composition of **HCR**. The ^1H NMR spectrum of (300 MHz, $CDCl_3$) showed a singlet at 2.42 ppm, which was assigned to methyl protons present in the coumarinyl backbone. The signals at δ 3.53–3.32 ppm were ascribed to methylene protons attached to nitrogen centres. The most deshielded protons at δ 8.62 ppm were assigned to imine protons, which confirmed the formation of a Schiff base. The triplet signal at δ 1.16 ppm indicated the presence of $-CH_3$ protons of the ethyl group. All other aromatic Hs were usual and were compared with literature data.[13,34] The C NMR spectrum was difficult to assign due to large number of overlapping C centres. Ester carbonyl and amide carbonyl appeared at 172.4 and 168.3 ppm, respectively. The peaks at 18.9 and 12.6 ppm were assigned to two types of methyl groups. Carbons attached to nitrogen centers appeared at 64.9, 53.5, 44.4, and 40.1 ppm. The quaternary carbon exhibited the highest δ value (64.9 ppm) among the above-mentioned four carbons and this was compared with the results of previous literature reports.[35]

3.2 Absorption spectroscopic studies

HCR exhibited absorption in ethanol-water (8 : 2, v/v; HEPES buffer, pH, 7.2) at 272, 317, 350 and 414 nm. The addition of following metal ions, for example, Na^+, K^+, Ca^{2+}, Mg^{2+}, Ba^{2+}, Al^{3+}, Mn^{2+}, $Fe^{2+/3+}$, Co^{3+}, Ni^{2+}, Cu^{2+}, Zn^{2+}, Cd^{2+}, Hg^{2+}, Ag^+, Pb^{2+}, and Pt^{2+} ($\approx 10^{-4}$ M) to **HCR** solution did not show any significant change in visible color under indistinguishable conditions; however, on adding Pd^{2+} at even lower concentrations ($\approx 10^{-6}$ to 10^{-5} M), we observed reasonable improvement in absorbance at 565 nm and a visible change in colour (Fig. 1). With the addition of Pd^{2+} to EtOH/H_2O solution (8 : 2, v/v, HEPES buffer, pH 7.2) of **HCR**, the pale yellow colour of the free probe changed to pink with a strong absorption band centered at 565 nm (Fig. 2). These results confirmed the unique selectivity of **HCR** to Pd^{2+} over other competitive metal ions; the experiment indicated that the probe is a simple sensitive naked-eye probe for Pd^{2+}.

3.3 Emission spectroscopic studies

The sensor **HCR** has two fluorogenic units, coumarin and rhodamine-B; therefore, we believe that it can be utilized as a powerful fluorogenic dyad. With the end goal of additionally exploring the selectivity of **HCR** to Pd^{2+}, the fluorescence spectral response of **HCR** to the previously mentioned metal ions was analyzed. On addition of Pd^{2+} to the solution of **HCR**, a brilliant fluorescence was observed (Fig. 3) at 598 nm with a high

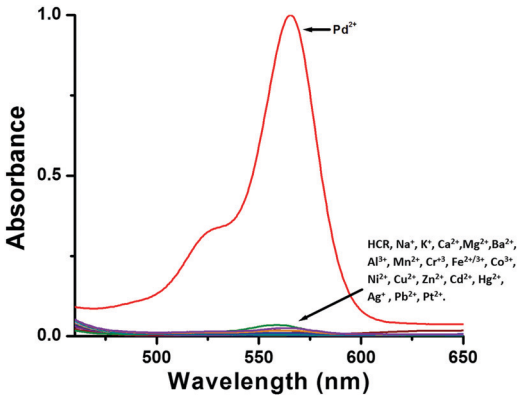

Fig. 1 UV-Vis responses of **HCR** to various metal ions in EtOH/H_2O (8 : 2, v/v, HEPES buffer, pH 7.2). [**HCR**] = 2.0 × 10^{-5} M, [Pd^{2+}] = 1.0 × 10^{-5} M, [other ions] ≈ 10^{-4} M.

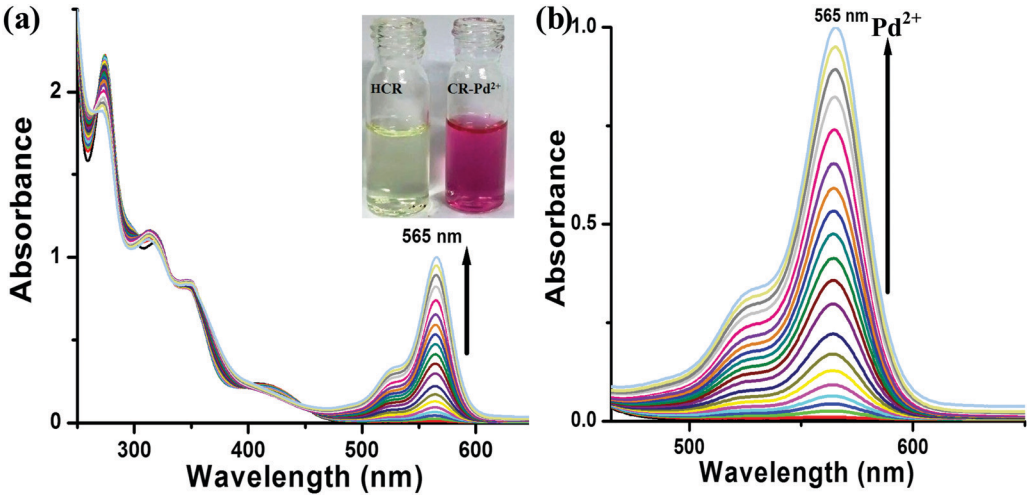

Fig. 2 (a) Variation of UV-Vis spectrum of sensor **HCR** (2.0×10^{-5} M) in EtOH/H_2O (8 : 2 v/v, 20 mM HEPES buffer, pH 7.2) medium on adding Pd^{2+} ions (0 to 9.5×10^{-5} M with increment of 5.0×10^{-7} M) gradually. (b) Magnification of the relevant portion of (a). Inset: Naked eye view of the sensor solution before and after addition of Pd^{2+} ions.

quantum yield of the $[\mathbf{CR}^{-}\text{-}Pd^{2+}]^{+}$ complex (Φ, 0.68; fluorescein standard), while **HCR** was very weakly emissive (Fig. 3). This demonstrated that **HCR** is extremely selective to Pd^{2+} ions. During titration of **HCR** solution by adding Pd^{2+} ions, the fluorescence intensity at 598 nm gradually increased; excitation at 545 nm enhanced the fluorescence intensity by 270 times (Fig. 4). The experimental detection limit (LOD) of Pd^{2+} was 18.8 nM (3σ method, ESI,† Fig. S5). Use of a number of rhodamine-functionalized sensors for quantitative identification of Pd^{2+} has been reported; for example, rhodamine-bonded azophenol showed LOD of 450 nM,[34] a rhodamine-nitro-salicyaldehyde Schiff base exhibited LOD of 50 nM,[19] rhodamine–ethynyl–benzaldehyde gave LOD of 191 nM,[35] rhodamine-appended oxime was reported with LOD of 15 nM,[36] and rhodamine-benzimidazole showed LOD of 21 nM.[37] The present probe **HCR** is astoundingly highly sensitive (LOD, 18.8 nM) and it is a potential competitor for other Pd^{2+} sensors.

The complex $[\mathbf{CR}^{-}\text{-}Pd^{2+}]^{+}$ showed better excited state stability ($\tau_{complex}$, 1.62 ns) than the free ligand **HCR** only (τ_{HCR}, 0.15 ns) (Fig. 5). Enhancement in lifetime on binding with Pd^{2+} supported stabilization at excited state by sharing orbitals of metal ions. Hence, Pd^{2+} induced cleavage of the C–O bond with consequent chelation and opening of the spirolactam ring[38–45] (Scheme 1).

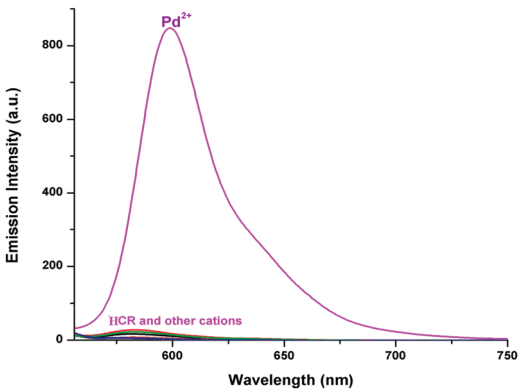

Fig. 3 Emission spectra of **HCR** after adding different metal ions and Pd^{2+} in EtOH/H_2O (8 : 2 v/v, 20 mM HEPES buffer, pH 7.2). [**HCR**] = 2.0×10^{-5} M, [Pd^{2+}] = 1.0×10^{-5} M, [other ions] ≈ 10^{-4} M.

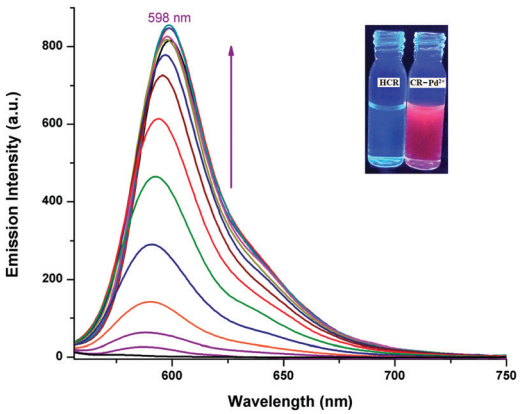

Fig. 4 Alteration in the fluorescence spectra of **HCR** upon addition of Pd^{2+} at an emission slit of 5 nm; inset: naked eye view of the sensor solution (placed in a UV chamber) in the presence and absence of Pd^{2+} ions.

pH sensitivity of the emission of **HCR** showed that there is almost no change in emissivity of the ligand in the pH range of 7.0–12.0; however, in acidic pH range of 3.0–7.0, a substantial intensity change was observed. In the presence of Pd^{2+}, the ligand did not show any change in emission in the pH range of 2.0–12.0 (Fig. 6). Hence, sensing of Pd^{2+} by **HCR** through fluorescence enhancement was most suitable in the pH range of 7.0–12.0, which may be attributed solely to spirolactam ring opening of the rhodamine moiety caused by Pd^{2+} ions. Thus, Pd^{2+} can be detected in approximately physiological pH ranges in living cells using **HCR**.

To further explore the selectivity of **HCR** for Pd^{2+}, competitive experiments were performed in the presence of Pd^{2+} mixed with 2.0 equiv. of each guest cation. Fig. 7 shows that these free

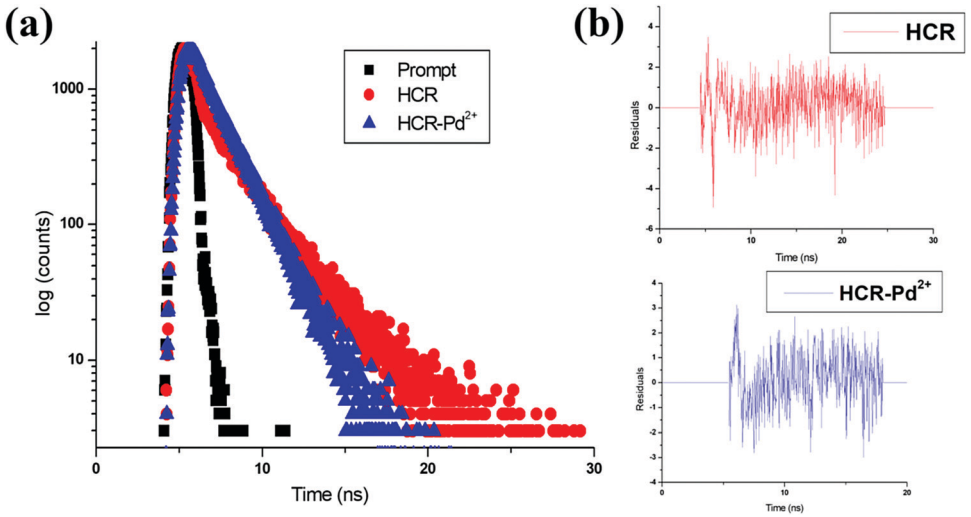

Fig. 5 (a) Time-resolved fluorescence decay of **HCR** in the absence and presence of Pd^{2+} in the medium already mentioned; (b) corresponding residual plot (λ_{ex} = 450 nm).

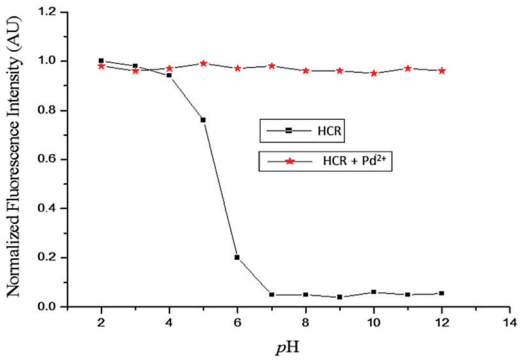

Fig. 6 Variation of normalized fluorescence intensity of (**HCR**) and [**CR**$^{-}$-Pd^{2+}]$^{+}$ in EtOH/H_2O (8 : 2, v/v) (λ_{ex} = 545 nm, λ_{em} = 598 nm) with change in pH.

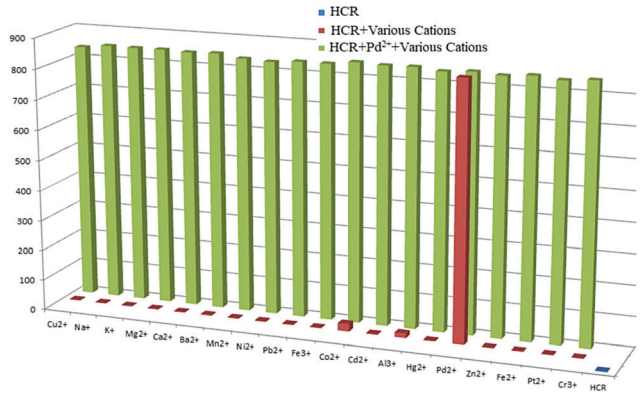

Fig. 7 Fluorescence intensity change of 20 μM **HCR** in EtOH/ H_2O (8 : 2, v/v) by Pd^{2+} ions at pH 7.2 in the presence of competing metal ions.

cations would have no such influence toward **HCR** and do not hamper the fluorogenic detection of Pd^{2+}. Thus, coexisting metal ions do not significantly influence the recognition of Pd^{2+} by **HCR**.

3.4 Proposed binding mode

From the absorption spectral data, Job's method of continuous variation yielded 1 : 1 (**HCR** : Pd^{2+}) stoichiometry for the complex (ESI,† Fig. S6). The association constant (K_a) of the sensor with Pd^{2+} ions was found to be 9.1 × 10^4 M^{-1} from Benesi–Hildebrand equation using emission titration data (ESI,† Fig. S7). In FTIR spectrum of the sensor, a broad peak at 3444 cm^{-1} for –OH (**HCR**) disappears for the complex [**CR**$^{-}$-Pd^{2+}]$^{+}$ (ESI,† Fig. S8), which refers to the binding of ligand to Pd(II) through the oxygen of –OH *via* deprotonation. In the ESI-MS experiment, free **HCR** showed a signal at m/z = 671.16 $[M + H]^{+}$; after completion of the reaction of Pd^{2+} with **HCR**, ESI-MS spectrum showed a clear base peak at 775.1075 $[M]^{+}$ (ESI,† Fig. S9), which certainly corresponded to the formation of the complex [**CR**$^{-}$-Pd^{2+}]$^{+}$. All these results suggested that the coordination cavity generated by the coumarinyl-rhodamine dyad with hydroxy-O and imine-N chelator caused binding of Pd^{2+}, resulting in the four-coordinated [**CR**$^{-}$-Pd^{2+}]$^{+}$ complex by inducing opening of the spirolactam ring (Scheme 1). It has been reported[45–48] that the opening of the spirolactam ring of rhodamine moiety enhances the emission intensity. This occurred due to the increase in conjugation in the ring-open form than in the ring-closed form, which decreased the HOMO–LUMO energy gap from the free sensor to its Pd(II) complex. Thus, the proposed mechanism will be as that shown in Scheme 1.

3.5 Theoretical studies

The geometry generated by DFT for [**CR**$^{-}$-Pd^{2+}]$^{+}$ was distorted square planar about Pd^{2+} ions, where **HCR** acted as an O, N, N, O chelator. The calculated Pd–O (rhodamine), Pd–N (imine), Pd–O (coumarinyl) and Pd–N (rhodamine) distances were 2.48, 1.97, 2.20 and 2.48 Å, respectively, which were comparable with those of a similar reported structure.[49,50] Upon coordination, the decrease in C–O (coumarinyl) distance from 1.38 to 1.32 Å was calculated; moreover, increase in the C–O (spirolactam) distance from 1.25 to 1.30 Å and that in the imine C═N

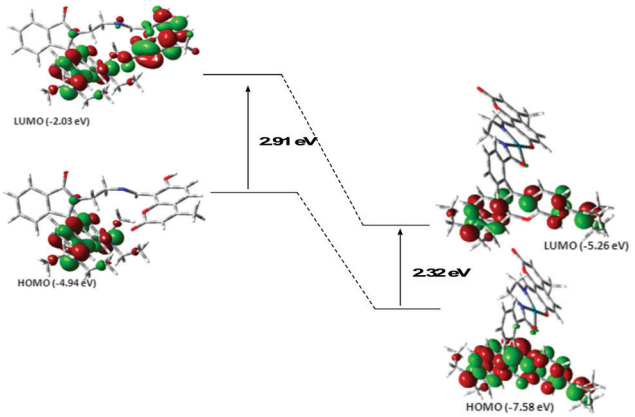

Fig. 8 HOMO–LUMO transitions of **HCR** and [**CR**$^{-}$-Pd^{2+}]$^{+}$ complex.

distance from 1.27 to 1.30 Å were calculated. On chelation of Pd^{2+} ions with **HCR**, the energy of HOMO and LUMO decreased relative to those of free **HCR** (ESI,† Fig. S1 and S2). The HOMO–LUMO energy gap in **HCR** was 2.91 eV (≡426 nm), while that for the complex [**CR**$^{-}$-Pd^{2+}]$^{+}$ was 2.32 eV (≡535 nm) (Fig. 8); these were in agreement with the experimentally observed longest wavelength absorption bands of **HCR** and [**CR**$^{-}$-Pd^{2+}]$^{+}$, respectively (Fig. 2). This supported the fact that the appearance of the intense 565 nm absorption band on addition of Pd^{2+} was due to the formation of an entirely new species, *i.e.*, the [**CR**$^{-}$-Pd^{2+}]$^{+}$ complex.

3.6 Intracellular imaging of Pd^{2+}

The above-mentioned experiments established the unique selectivity and extreme sensitivity of **HCR** to Pd^{2+} with very low detection limit (18.8 nM); we were interested in verifying the potential utility of the sensor for living cells. Therefore, we first checked the toxicity of the ligand in MCF-7 (breast cancer cell line) upto 200 μM. The sensor showed toxicity after 25 μM (Fig. 9) and could be used as an anticancer agent. After the fluorescence microscopic technique, the detection of Pd^{2+} at a very low concentration was examined in living cells. Palladium (0, II, IV) is a useful catalyst in organic synthesis and the final product may contain traces of Pd(II) even after thorough repeated purification. Such contamination of Pd is known to cause

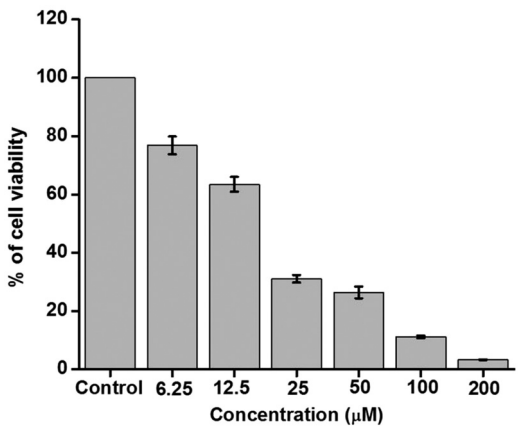

Fig. 9 Cell viability test by MTT assay by adding **HCR** to the media.

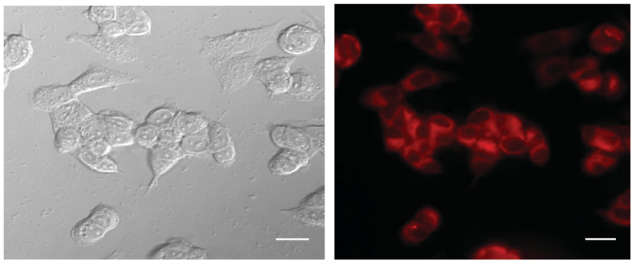

Fig. 10 Images of MCF7 cells after the treatment with compound with Pd^{2+}.

irritation of skin, eyes, and respiratory tract; moreover, Pd(II) complexes are reportedly toxic and carcinogenic.[51] For Pd, with a lethal dose of 5–10 ppm,[51–53] the WHO recommendation for maximum uptake is restricted to ~1.5–15 μg per day. Thus, the development of a highly specific Pd^{2+} detection technique in living cells is an important requirement of current research. In the present work, cells were incubated with 5.0 μM of **HCR** for 3 h at 37 °C and then treated with $PdCl_2$ (5 μM) for 30 min at the same temperature, which resulted in red fluorescence (Fig. 10). The red emission indicated that **HCR** easily entered the cell membrane and was capable of imaging Pd^{2+} in living cells. Therefore, it may be concluded that in both *in vitro* sensing and *in vivo* sensing and in whole cell imaging of Pd^{2+}, **HCR** is a potential analytical reagent. Moreover, a control experiment was performed to check whether the spiro ring remained intact in the cell culture medium. The cells were treated with **HCR** (5 μM) for 24 h but did not show any sign of red coloration. This result suggests that even in a complicated biological medium, the spiro ring of **HCR** does not open (ESI,† Fig. S10).

4. Conclusion

The synthesized coumarinyl-rhodamine dyad (**HCR**) served as a highly efficient fluorescent sensor (λ_{em}, 598 nm) for the quantitative detection of Pd^{2+} in a semi-aqueous solution in the presence of many other metal ions with a very low detection limit of 18.8 nM. The selectivity was demonstrated using fluorescence, absorption and mass spectroscopies. The fluorescence intensity of the sensor enhanced 270-fold by adding Pd^{2+} *via* opening of ring of the spirolactam form of rhodamine moiety. This sensor acted as a dual probe for visually detecting Pd^{2+} ions *via* change in fluorescence and color. Due to high selectivity of **HCR** to Pd^{2+} in a physiological medium at an intracellular level, it can be used for the identification of breast cancer cells.

Conflicts of interest

There are no conflicts to declare.

Acknowledgements

Financial support from the Council of Scientific and Industrial Research (CSIR, Sanction No. 01(2814)/17/EMR-II), New Delhi,

India is gratefully acknowledged. Dr Madhumita Manna, Principle, Bidhannagar College has acknowledged for her enormous moral support and encouragement. One of the authors (R. P.) is thankful to Department of Science and Technology (DST), Govt of India for providing DST-INSPIRE research fellowship.

References

1 (*a*) L. Pu, *Chem. Rev.*, 2004, **104**, 1687–1716; (*b*) V. Amendola, L. Fabbrizzi, F. Forti, M. Licchelli, C. Mangano, P. Pallavicini, A. Poggi, D. Sacchi and A. Taglieti, *Coord. Chem. Rev.*, 2006, **205**, 273–299; (*c*) E. M. Nolan and S. J. Lippard, *Chem. Rev.*, 2008, **108**, 3443–3480.

2 (*a*) J. F. Zhang, Y. Zhou, J. Yoon and J. S. Kim, *Chem. Soc. Rev.*, 2011, **40**, 3416–3429; (*b*) Z. Xu, X. Chen, H. N. Kim and J. Yoon, *Chem. Soc. Rev.*, 2010, **39**, 127–137; (*c*) R. Balamurugan, C. C. Chien, K. M. Wu, Y.-H. Chiu and J.-H. Liu, *Analyst*, 2013, **138**, 1564–1569.

3 (*a*) H. Kim, K. S. Moon, S. Shim and J. Tae, *Chem. – Asian J.*, 2011, **6**, 1987–1991; (*b*) H. Li, J. Fan, J. Du, K. Guo, S. Sun, S. Liu and X. Peng, *Chem. Commun.*, 2010, **46**, 1079–1081.

4 (*a*) H. Li, J. Fan, F. Song, H. Zhu, J. Du, S. Sun and X. Peng, *Chem. – Eur. J.*, 2010, **16**, 12349–12356; (*b*) D. Keum, S. Kim and Y. Kim, *Chem. Commun.*, 2014, **50**, 1268–1270.

5 (*a*) M. Ware, *Platinum Met. Rev.*, 2005, **49**, 190–195; (*b*) T. Iwasawa, M. Tokunaga, Y. Obora and Y. Tsuji, *J. Am. Chem. Soc.*, 2004, **126**, 6554–6555; (*c*) K. Köhler, W. Kleist and S. S. Pröcki, *Inorg. Chem.*, 2007, **46**, 1876–1879; (*d*) C. M. Crudden, M. Sateesh and R. Lewis, *J. Am. Chem. Soc.*, 2005, **127**, 10045–10050.

6 (*a*) S. L. Buchwald, C. Mauger, G. Mignani and U. Scholzc, *Adv. Synth. Catal.*, 2006, **348**, 23–29; (*b*) X. Chen, K. M. Engle, D. H. Wang and J. Q. Yu, *Angew. Chem.*, 2009, **212**, 5196–5217.

7 (*a*) J. Kielhorn, C. Melber, D. Keller and I. Mangelsdorf, *Int. J. Hyg. Environ. Health*, 2002, **205**, 417–432; (*b*) C. D. Spicer, T. Triemer and B. G. Davis, *J. Am. Chem. Soc.*, 2012, **134**, 800–803.

8 T. Gebel, H. Lantzsch, K. Plebow and H. Dunkelberg, *Mutat. Res., Genet. Toxicol. Environ. Mutagen.*, 1997, **389**, 183.

9 T. Z. Liu, S. D. Lee and R. S. Bhatnagar, *Toxicol. Lett.*, 1979, **4**, 469–473.

10 J. Kielhorn, C. Melber, D. Keller and I. Mangelsdorf, *Int. J. Hyg. Environ. Health*, 2002, **205**, 417–432.

11 B. Dimitrova, K. Benkhedda, E. Ivanova and F. Adams, *J. Anal. At. Spectrom.*, 2004, **19**, 1394–1396.

12 C. Locatelli, D. Melucci and G. Torsi, *Anal. Bioanal. Chem.*, 2005, **382**, 1567–1573.

13 K. Van Meel, A. Smekens, M. Behets, P. Kazandjian and R. Van Grieken, *Anal. Chem.*, 2007, **79**, 6383–6389.

14 (*a*) H. Li, J. Fan and X. Peng, *Chem. Soc. Rev.*, 2013, **42**, 7943–7962; (*b*) J. Du, M. Hu, J. Fan and X. Peng, *Chem. Soc. Rev.*, 2012, **41**, 4511–4535.

15 (*a*) L. Duan, Y. Xu and X. Qian, *Chem. Commun.*, 2008, 6339–6341; (*b*) J. R. Matthews, F. Goldoni, H. Kooijman, A. L. Spek, A. P. H. J. Schenning and E. W. Meijer, *Macromol. Rapid Commun.*, 2007, **28**, 1809–1815.

16 (*a*) A. K. Mahapatra, S. K. Manna, K. Maiti, S. Mondal, R. Maji, D. Mandal, S. Mandal, M. R. Uddin, S. Goswami, C. K. Quah and H. Fun, *Analyst*, 2015, **140**, 1229–1236; (*b*) S. Goswami, D. Sen, N. K. Das, H. Fun and C. K. Quah, *Chem. Commun.*, 2011, **47**, 9101–9103.

17 G. Wei, L. Wang, J. Jiao, J. Hou, Y. Cheng and C. Zhu, *Tetrahedron Lett.*, 2012, **53**, 3459–3462.

18 (*a*) Y. K. Yang, K. J. Yook and J. Tae, *J. Am. Chem. Soc.*, 2005, **127**, 16760–16761; (*b*) J. Y. Kwon, Y. J. Jang, Y. J. Lee, K. M. Kim, M. S. Seo, W. Nam and J. Yoon, *J. Am. Chem. Soc.*, 2005, **127**, 10107–10111; (*c*) V. Dujols, F. Ford and A. W. Czarnik, *J. Am. Chem. Soc.*, 1997, **119**, 7386–7387; (*d*) M. Wang, X. Liu, H. Lu, H. Wang and Z. Qin, *ACS Appl. Mater. Interfaces*, 2015, **7**, 1284–1289; (*e*) R. Balamurugan, J.-H. Liu and B.-T. Liu, *Coord. Chem. Rev.*, 2018, **376**, 196–224; (*f*) N. Kumari, N. Dey, K. Kumar and S. Bhattacharya, *Chem. – Asian J.*, 2014, **9**, 3174–3181; (*g*) H. Li, J. Cao, H. Zhu, J. Fan and X. Peng, *Tetrahedron Lett.*, 2013, **54**, 4357–4361.

19 A. K. Bhanja, S. Mishra, K. Das Saha and C. Sinha, *Dalton Trans.*, 2017, **46**, 9245–9252.

20 A. K. Bhanja, S. Mishra, K. Kar, K. Naskar, S. Maity, K. Das Saha and C. Sinha, *New J. Chem.*, 2018, **42**, 17351–17358.

21 J. Q. Umberger and V. K. LaMer, *J. Am. Chem. Soc.*, 1945, **67**, 1099–1109.

22 K. Das, U. Panda, A. Datta, S. Roy, S. Mondal, C. Massera, T. Askun, P. Celikboyun, E. Garribba, C. Sinha, K. Anand, T. Akitsu and K. Kobayashi, *New J. Chem.*, 2015, **39**, 7309–7321.

23 J.-S. Wu, I.-C. Hwang, K. S. Kim and J. S. Kim, *Org. Lett.*, 2007, **9**, 907–910.

24 M. J. Frisch, G. W. Trucks, H. B. Schlegel, G. E. Scuseria, M. A. Robb, J. R. Cheeseman, G. Scalmani, V. Barone, B. Mennucci, G. A. Petersson, H. Nakatsuji, M. Caricato, X. Li, H. P. Hratchian, A. F. Izmaylov, J. Bloino, G. Zheng, J. L. Sonnenberg, M. Hada, M. Ehara, K. Toyota, R. Fukuda, J. Hasegawa, M. Ishida, T. Nakajima, Y. Honda, O. Kitao, H. Nakai, T. Vreven, J. A. Montgomery Jr., J. E. Peralta, F. Ogliaro, M. Bearpark, J. J. Heyd, E. Brothers, K. N. Kudin, V. N. Staroverov, R. Kobayashi, J. Normand, K. Raghavachari, A. Rendell, J. C. Burant, S. S. Iyengar, J. Tomasi, M. Cossi, N. Rega, J. M. Millam, M. Klene,J. E. Knox, J. B. Coss, V. Bakken, C. Adamo, J. Jaramillo, R. Gomperts, R. E. Stratmann, O. Yazyev, A. J. Austin, R. Cammi, C. Pomelli, J. W. Ochterski, R. L. Martin, K. Morokuma, V. G. Zakrzewski, G. A. Voth, P. Salvador, J. J. Dannenberg, S. Dapprich, A. D. Daniels, Ö. Farkas,J. B. Foresman, J. V. Ortiz, J. Cioslowski and D. J. Fox, *Gaussian 09, Revision D.01*, Gaussian Inc., Wallingford, CT, 2009.

25 A. D. Becke, *J. Chem. Phys.*, 1993, **98**, 5648–5652.

26 C. Lee, W. Yang and R. G. Parr, *Phys. Rev. B: Condens. Matter Mater. Phys.*, 1988, **37**, 785–789.

27 P. J. Hay and W. R. Wadt, *J. Chem. Phys.*, 1985, **82**, 270–283.

28 W. R. Wadt and P. J. Hay, *J. Chem. Phys.*, 1985, **82**, 284–298.

29 P. J. Hay and W. R. Wadt, *J. Chem. Phys.*, 1985, **82**, 299–305.

30 V. Barone and M. Cossi, *J. Phys. Chem. A*, 1998, **202**, 1995–2001.
31 M. Cossi and V. Barone, *J. Chem. Phys.*, 2001, **115**, 4708–4717.
32 M. Cossi, N. Rega, G. Scalmani and V. Barone, *J. Comput. Chem.*, 2003, **24**, 669–681.
33 N. M. O'Boyle, A. L. Tenderholt and K. M. Langner, *J. Comput. Chem.*, 2008, **29**, 839–845.
34 A. K. Mahapatra, S. K. Manna, K. Maiti, S. Mondal, R. Maji, D. Mandal, S. Mandal, M. R. Uddin, S. Goswami, C. K. Quah and H. K. Fun, *Analyst*, 2015, **140**, 1229–1236.
35 F. Liu, J. Du, M. Xu and G. Sun, *Chem. – Asian J.*, 2016, **11**, 43–48.
36 Q. Huang, Y. Zhou, Q. Zhang, E. Wang, Y. Min, H. Qiao, J. Zhang and T. Ma, *Sens. Actuators, B*, 2015, **208**, 22–29.
37 Y. Chen, B. Chen and Y. Han, *Sens. Actuators, B*, 2016, **237**, 1–7.
38 V. Sharma, A. K. Sainib and S. M. Mobin, *J. Mater. Chem. B*, 2016, **4**, 2466–2476.
39 J. Panchompoo, L. Aldous, M. Baker, M. I. Wallace and R. G. Compton, *Analyst*, 2012, **137**, 2054–2062.
40 W. Liu, J. Jiang, C. Chen, X. Tang, J. Shi, P. Zhang, K. Zhang, Z. Li, W. Dou, L. Yang and W. Liu, *Inorg. Chem.*, 2014, **53**, 12590–12594.
41 F. Song, A. L. Garner and K. Koide, *J. Am. Chem. Soc.*, 2007, **129**, 12354–12355.
42 D. Keum, S. Kim and Y. Kim, *Chem. Commun.*, 2014, **50**, 1268–1270.
43 P. Kumar, V. Kumar and R. Gupta, *RSC Adv.*, 2017, **7**, 7734–7741.
44 W. X. Ren, T. Pradhan, Z. Yang, Q. Y. Cao and J. S. Kim, *Sens. Actuators, B*, 2012, **171**, 1277–1282.
45 S. Sun, B. Qiao, N. Jiang, J. Wang, S. Zhang and X. Peng, *Org. Lett.*, 2014, **16**, 1132–1135.
46 S. Goswami, D. Sen, N. Kumar Das, H. K. Fun and C. K. Quahb, *Chem. Commun.*, 2011, **47**, 9101–9103.
47 M. A. Bennett, S. K. Bhargava, M. A. Keniry, S. H. Privér, P. M. Simmonds, J. Wagler and A. C. Willis, *Organometallics*, 2008, **27**, 5361–5370.
48 U. G. Reddy, F. Ali, N. Taye, S. Chattopadhyay and A. Das, *Chem. Commun.*, 2015, **51**, 3649–3652.
49 B. Liu, H. Wang, T. Wang, Y. Bao, F. Du, J. Tian, Q. Li and R. Bai, *Chem. Commun.*, 2012, **48**, 2867–2869.
50 X. Wang, Z. Guo, S. Zhu, H. Tian and W. Zhu, *Chem. Commun.*, 2014, **50**, 13525–13528.
51 C. E. Garrett and K. Prasad, *Adv. Synth. Catal.*, 2004, **346**, 889–900.
52 D. G. Cho and J. L. Sessler, *Chem. Soc. Rev.*, 2009, **38**, 1647–1662.
53 F. Song, A. L. Garner and K. Koide, *J. Am. Chem. Soc.*, 2007, **129**, 12354–12355.

